Modelling Spudcan penetration using Abaqus CEL method

Aleksander Worren[1*]

[1]Technical Norwegian Geotechnical Institute, department of computational geomechanics, Oslo

ABSTRACT

A hazard during installation of jack-up spudcans is punch-through, which is characterized by a peak resistance, followed by a significant reduction in spudcan resistance. This might lead to an uncontrolled rapid leg penetration as the installation generally is load-controlled. The problem is typical for sites where a stiff soil layer is overlying a soft clay layer. Accurate calculation of the expected displacement-resistance curve for these soil conditions is therefore important in order to reduce the risk of uncontrolled punch-through conditions.

Numerical simulation of spud-can penetration into seabed during installation of jack-up platforms is a complex problem involving both large strains and large displacements where the geometry changes during penetration e.g. interface between layers. The Coupled-Eulerian-Lagrangion (CEL) method available in the finite element program package ABAQUS is suitable for this type of problem. The main aim of this Master Thesis is therefore to use the CEL method to analyse some published examples of spudcan penetration.

Keywords: Spudcan, Offshore, Abaqus, CEL,

1. INTRODUCTION

Jack-up rigs are the most common type of mobile platforms. They operate at shallow and up to moderate depths (167 meters (World Fleet of Jack-Up Drilling Rigs, 2012)). The spudcan may be penetrated up to tens of meters into the seabed if the soil is soft. The installation is performed by applying vertical load from the jack-rig and water ballast in the hull.

Jack-up rigs have movable legs, which may be jacked down into the seabed to give stabilization under operation, hence the name jack-up. The legs often stand on spudcan foundations, which are steel conical footings. Spudcans have a diameter of 10 to around 20 meters. The main objective to the spudcan is to distribute the load from the jack-up rig and give stability. The spudcan may be penetrated up to tens of meters into the seabed if the soil is soft. The installation is performed by applying vertical load from the jack-rig and water ballast in the hull. This means that the penetration is load controlled, and the average penetration rate is often around 1m/hour (Tjahyono, 2011).

The legs and jack-up rig may be damaged if the penetration rate becomes too large. It is therefore important to know the soil

* presenting author

characterization and expected load-response curve. A typical hazard is punch-through during the installation. It is characterized by a peak resistance during the installation, followed by a fast reduction in spudcan resistance. This might lead to a rapid penetration because the installation is load-controlled. This problem is typical for sites where a stiff soil layer is overlying a soft clay layer. Punch-trough of a jack-up leg will cause the platform to tilt which consequently will give rise to large bending moments. The bending moment may lead to failure in the jack-up legs and connection between the legs and rig. This can endanger personnel and result in huge economic loss.

The main aim of this master thesis is to use the CEL method in Abaqus/Explicit to analyze some published examples of spudcan-penetration. Special focus will be to consider the effect of large strain in clay, e.g. gradual reduction of the undrained shear strength with increasing strain.

2. THEORY

All of the finite element calculations will be executed in Abaqus/Explicit.

2.1. Coupled Eulerian-Lagrangian

Lagrangian elements have material fixed to the nodes. As a result, the elements will deform as the material deforms. This may lead to numerical problems in large deformation problems. Heavily distorted elements will not work well, and problems like mesh locking, and numerical instability can follow.

In eulerian element formulation, the nodes are fixed in space (coordinate system), while the material is free to move (flow) through the mesh (Abaqus 6.12 Analysis User's Manual). The mesh will consequently not deform as the material deforms. Figure 2-1 shows the deformation of a lagrangian mesh over the deformation of a eulerian mesh. This is particularly useful when dealing with large deformation, where the lagrangian elements would get heavily distorted and encounter numerical problems.

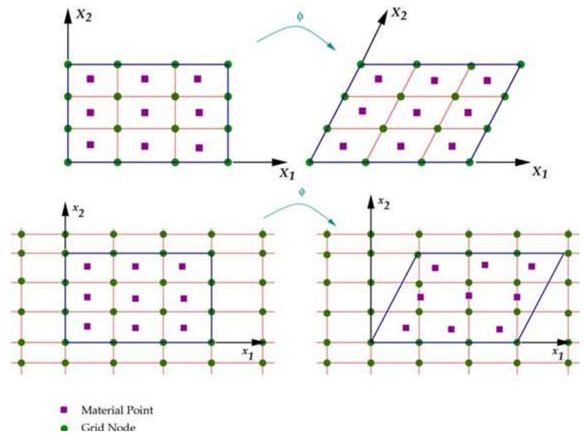

Figure 2-1 Lagrangian element deformation on the top, and eulerian deformation at the bottom. (Nonlinear finite elements/Lagrangian and Eulerian descriptions, 2010)

It is possible to have more than one material in the eulerian mesh using Abaqus/Explicit. The materials are assigned using initial conditions in the start of the analysis. The elements are by default empty (volume fraction = 0), while the volume fraction is one when the element is completely filled with material (Figure 2-2). The material is tracked as it moves through the mesh by calculating the eulerian volume fraction (EVF) of each element. The eulerian material will disappear from the simulation if it moves outside the mesh. The material boundaries (interfaces) are tracked using the computed eulerian volume fraction by each incrementation. Abaqus/Explicit uses an interface reconstruction algorithm that approximates a planar boundary within each element (Abaqus 6.12 Analysis User's Manual). The simplification with planar boundary may lead to discontinues in the interfaces if a coarse mesh is used.

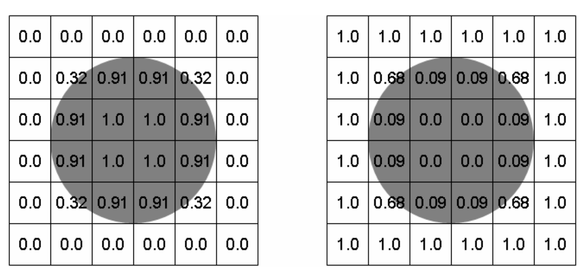

Figure 2-2 Volume fractions (Abaqus/CAE User's Manual)

2.2. T-bar penetration

The preliminary analyses included T-bar penetration tests.

The T-bar penetration test is similar to the CPT (Cone Penetration Test) except that it is a horizontal cylinder that is pushed through the soil. It is used to define the cohesion for soft clays. The resistance is measured during the penetration, and the undrained resistance force is calculated.

$$\frac{P}{s_u d} = N_b$$

P is the force per unit length acting on the cylinder, s_u is the undrained shear strength, *d* is the diameter of the cylinder, and N_b is the bar factor. The bar factor is dependent on the roughness of the cylinder. The theoretical value is approximately 12 for rough contact, and 9 for smooth contact (Randolph, M.F. & Houlsby, G.T., 1984) (Stewart, D.P. & Randolph, M.F., 1994). This factor is theoretical, and is based on a plastic solution with a soil model which is elastic-perfectly plastic. Effects like strain-rate dependency, strain-softening and anisotropy are not included. Strain-rate dependency and strain-softening is shown to have a significant effect on the bar factor (Liyanapathirana, 2008), while the bar factor is relatively insensitive to anisotropy (Randolph, M.F. & Andersen, K.H., 2006).

3. RESULTS

3.1. T-bar test

First a mesh convergence test was performed in order to study the effect of the element size for soil-flow around the T-bar. The speed of the T-bar was not studied in these analyses, and it is not the same for all the models. It might, however, have been more efficient to study the speed of the T-bar in advance in order to know which speed to use to avoid oscillations in the result.

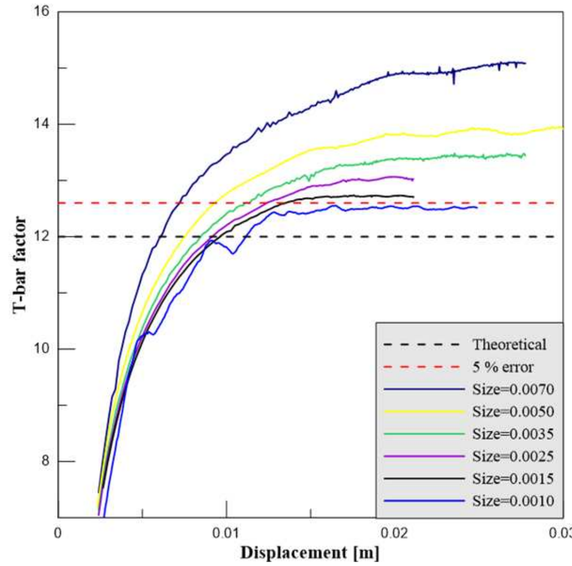

Figure 3-1 Mesh convergence for the T-bar test

The calculations show that the T-bar factor is significantly affected by the element size. Convergence to a constant value was not possible as the calculation time become too great for smaller element size. However, the models with the smallest element size performed well, and the error for element size 0.0010 is less than 5 %.

The flow around the T-bar displays why the models with denser mesh give less resistance and therefor more accurate results. In Figure 3-2 is the flow pattern of the model with element size 0.0015 displayed over the model with element size 0.0070. A smaller amount of soil flow around the T-bar in the model with denser mesh, and consequently less resistance is measured. The edge of the soil that flows around the T-bar is located 0.05 meters from the side of the T-bar for element size 0.0015, while the distance is 0.07 meters for element size 0.0070. The shear band which is established along the edge of the soil flow is also narrower and more distinct for smaller element size (Figure 3-3), which will result in lower resistance.

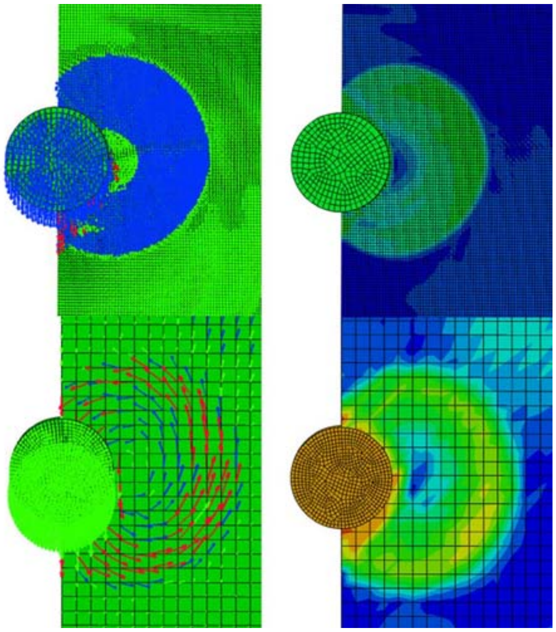

Figure 3-2 Flow: element size 0.0015 and 0.0070

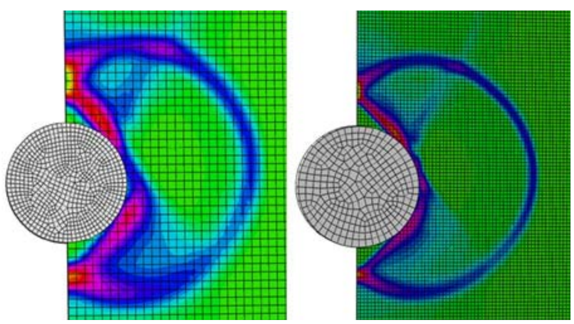

Figure 3-3 Shear bands, Element size 0.0035 and 0.0015

The mesh convergence test indicated that the penetration speed affected how much oscillation that occurs in the results. It is also of interest to see if the bar factor changes for increased speed, or if the oscillations may be smoothed out (in order to get the right value). This is important to know for the spudcan penetration test, as the deformations are much greater, and increased speed may reduce the calculation time significantly. The model with element size 0.0015 was used for this study, and the speed is constant for each analysis. Several different speeds of penetration were tested, and a selection of two of them is shown in Figure 3-4.

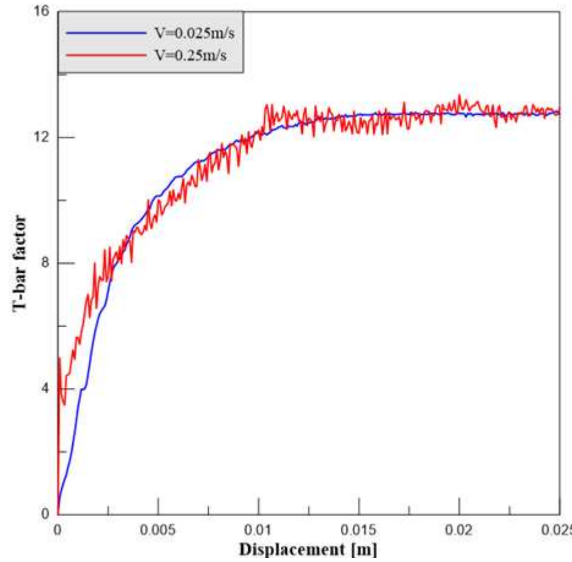

Figure 3-4 Speed convergence

The result indicates that the resistance is more influenced by the speed at small deformations than large deformations. The fast calculation seem to stabilize around the right value as the deformation become larger (>0.005 meters). And a T-bar factor with only a minor error is possible to obtain by filtering out the oscillations in the resistance for the fast calculation, for example by taking the average resistance over a given displacement. This approach may be used for the spudcan penetration analysis, as the deformation is large. However, it will lead to some errors if the resistance changes a lot during the penetration which may be the case around the punch-through depth.

3.2. Spudcan penetration

H/B refferes to the height of the first layer divided by the diameter of the spudcan, while D is the penetration depth.

Single layer

The first analysis on spudcan penetration was executed in order to verify the method. The soil is weightless in this case, so that none back-flow occurs. The spudcan is modeled as a flat cylinder with a rough base. The diameter of the cylinder is 15 meters. All the penetrations are preformed undrained, and poisons ratio of 0.495 is used. The cohesive yield strength is 10kPa for all the soil. Only 45 degrees of the problem is modeled, and symmetry boundary conditions are used on the sides. The height of the initially active elements (soil) is 3.5D=52.5 meters, while the radius is 2.5B=37.5 meters. Approximately 228 000 elements were used, and a penetration rate of 1m/s.

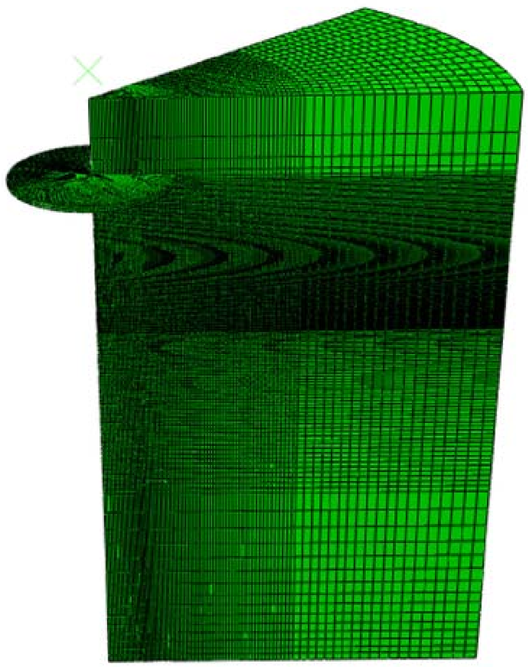

Figure 3-5 Mesh: single-layer penetration

The reaction force was measured, and oscillations were filtered out. The bearing capacity factor were calculated by $N=q/c_u$. The results were compared with Martin and Randolph's lower and upper bound solutions (Martin, C.M. and Randolph, M.F., 2001).

The calculation is in reasonable agreement with Martin & Randolph's bearing capacity theory. The result shows some error for shallow penetration, which is likely due to the dynamic inertia effects, or not small enough elements.

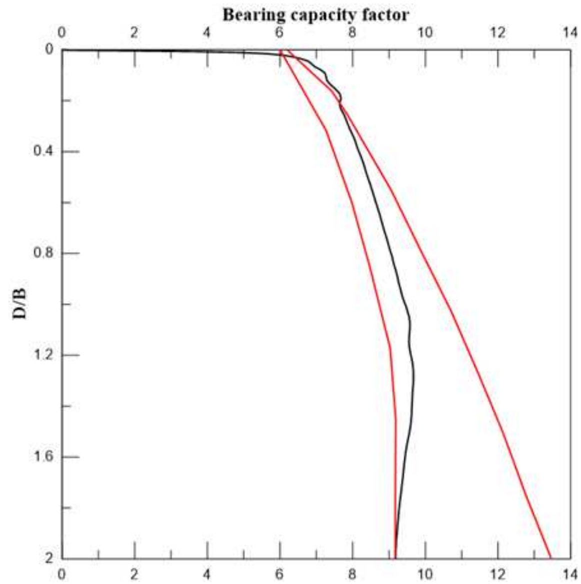

Figure 3-6 Bearing capacity factor for single-layer clay

Spudca penetation in two-layered clay

First, a case with no strain-softening was calculated, where the cohesive yield strength in the upper layer is 100kPa, and 20 kPa in the lower layer. The Young's modulus is $500c_u$, and the effective soil weight is $8.5kN/m^3$ for the upper layer and $7kN/m^3$ for the lower layer. The diameter of the spudcan is 15 meters. The case was found in Tjahyono's doctor thesis (Tjahyono, S. 2011).

The "decimateFilter" function in Abaqus/Explicit was used to filter out the oscillations in the test data. The results are shown in Figure 3-7, where the spudcan resistance is plotted against the normalized penetration H/B. It is evident that the oscillations are large in the beginning of the penetration. However, the result is not necessarily inaccurate. After filtering out the oscillations and comparing the resistance with Tjahyono's result, we get the result as shown in Figure 3-8. The result seem to be fairly good, in the sense that it does not deviate much from Tjayhono's FEM calculation, with the exception of the dynamic oscillations at the beginning, and at the end where backflow initiates. The deviation is at maximum around 25 kPa, for both the beginning and end of the penetration. The back-flow is initiated at around D/B=1.40, and the flow pattern and material boundaries are shown in Figure 3-9. The right picture shows the upper material in red and the lower material in blue. The eulerian mesh seem to preform very well in managing the boundaries, as we can see the upper layer is pushed into the lower layer.

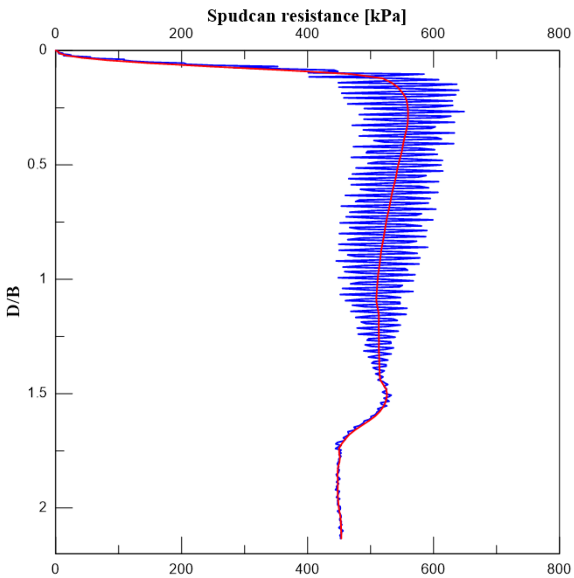

Figure 3-7 Response filter

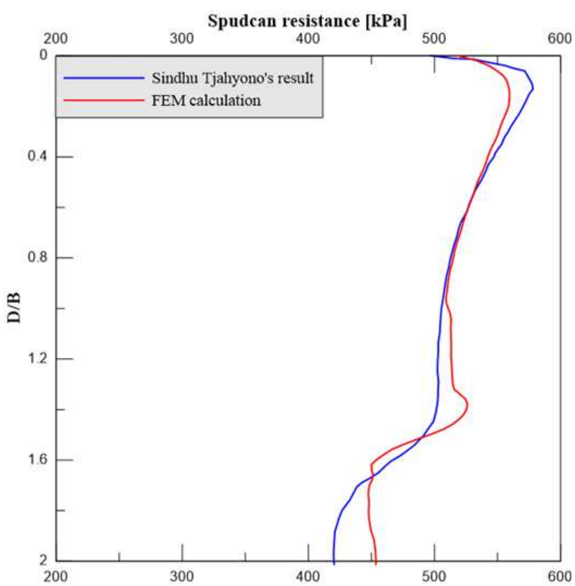

Figure 3-8 Spudcan resistance non-soft material, compared with Tjahyono's result

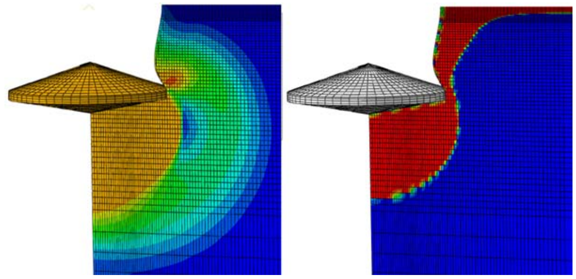

Figure 3-9 Flow pattern and material boundaries at initiation of back-flow (D/B ≈ 1.4).

The result from FEM calculation was also compared with the theoretical solutions from SNAME (2002), Hossain & Randolph and Tjahyono (2009) in Figure 3-10. The SNAME method overestimates the potential for punch-through, and underestimates the spudcan resistance. The reason for the apparently bad performance of SNAME method is because of the whished-in-place approach. This case involves a large reduction in the cohesive yield strength from the upper to the lower layer, and SNAME will consequently underestimate the resistance and overestimate the potential for punch-through as it does not account for the geometric chances in the soil. The much stronger upper layer will be pushed into the lower layer, and this deformation will increase the spudcan resistance and reduce the potential for punch-through. Hossain & Randolph's method performed better, but is still underestimating the spudcan resistance if we compare to the FEM calculation and Tjahyono's (2011) result. The FEM calculation is close to Tjahyono's theory (two different results is presented, as it was some uncertainties in the back-flow depth). The resistance is dependent on the element size for flow around an object as shown in the T-bar test, and from the comparison with Tjahyono's numerical and theoretical work is it possible to conclude that the elements are too large in the lower layer. However, the error was within acceptable range, and further reduction in element size would increase the calculation time which was already relatively long. The same mesh was therefore used for the rest of the calculations.

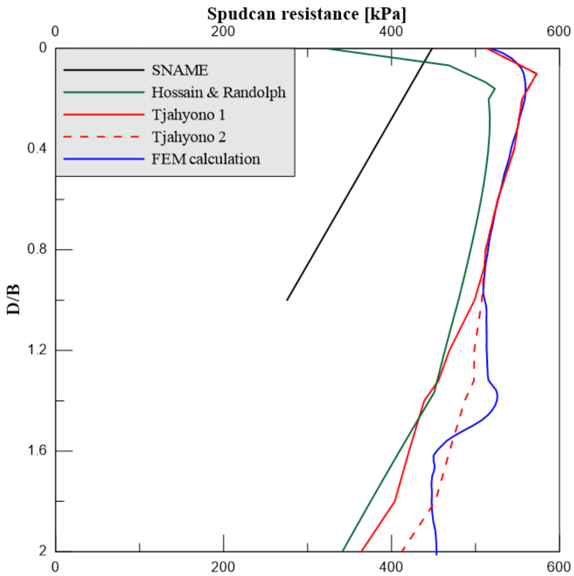

Figure 3-10 Comparison of spudcan resistance with hand calculations

Finally, strain-softening was implemented in the spudcan penetration test. Only the upper layer was subject to softening. The sensitivity of the soil was 2, which means that the softened soil have half the strength of the original soil. The absolute plastic strain for which the reduced cohesive yield strength was established varied from 2% to 20%. The upper bound solution ($c_{u1} = 100kPa$) and lower bound solution ($c_{u1} = 50kPa$) were also plotted in the result.

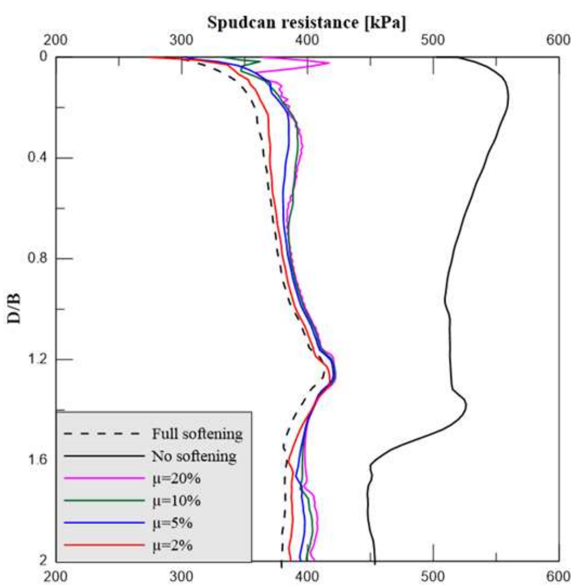

Figure 3-11 H/B=1. Spudcan resistance with strain-softening behavior

The results are plotted in Figure 3-11. All the calculations are pretty similar to the lower bound solution. It is suspected that this is due to that the shear bands are established at relative shallow penetration depth. The strain-softening behavior has less effect when the shear bands are established. This is due to the fact that the strains in the shear bands are much greater than the absolute plastic strain for which the soil is softened (μ). The models with μ=10% and μ=20% showed a spike in the resistance for shallow penetration depth ($D/B \approx 0.025$), but follow close to the lower limit for the rest of the penetration. The spike in resistance may be because the shear bands have yet to be established for the shallow penetration.

The depth of initiated backflow is similar for all the models, except for the upper bound solution. The depth is between D/B=1.1 and D/B=1.21 for the softened soil and lower bound solution, while it is between D/B=1.37 and D/B=1.47 for the upper bound solution. The depth of initiated backflow is a bit inaccurately determined because the output frames of the deformation are a bit too scarce.

Strain-softening may increase the punch-through danger. Indication of this can be observed for the calculation with μ=20%, the punch-through danger is greater than for the lower bound solution. Strain-softening is therefore an important parameter in the material model. However, these calculations are hard to interpret because of the dependency of the element size regarding the shear band thickness. It would be interesting to know how large μ (absolute plastic strain for the softened condition) is needed to increase the punch-through potential drastically. It seems to be between 10-20% for this analysis, but it is not possible to conclude this, as a different mesh would probably give a different result. But Tjahyono's result showed a similar result, and it was concluded that μ < 5% could be calculated using the lower bound solution (no strain-softening), while this is not possible for μ > 5%.

4. CONCLUSIONS

The CEL method in Abaqus/Explicit has proven to be suitable for spudcan penetration problems. The penetration speed affected mainly how much oscillation that occurs in the results. The oscillation may be filtered out as the resistance oscillated around a mean value. The computational cost for these types of problems are large, and it is therefore of interest to find the highest penetration rate for which oscillations may be filtered out. However, there were some difficulties regarding the effects from the element size, especially when trying to include strain-softening behavior. It is important to address this problem, as non-conservative results might be obtained.

ACKNOWLEDGEMENTS

I would like to thank Dr. Hans Petter Jostad for guidance trouhout the master thesis. I would also like to thank Dr. Khoa Huyan for learning me how to model spudcan penetration using the CEL method in Abaqus/Explicit.

REFERENCES

Abaqus 6.12 Analysis User's Manual. (n.d.). Eulerian Analysis, Chapter 14.1.

Abaqus/CAE User's Manual. (n.d.). The volume fraction tool, Chapter 28.5.

Hossain, M.S. & Randolph, M.F. (2009). New mechanism-based design approach for spudcan foundations on stiff-over-soft clay. Offshore Technology Conference. Houston.

Liyanapathirana, D. M. (2008). Numerical simulation of T-bar penetration in soft clay. GeoCongress.

Martin, C.M. and Randolph, M.F. (2001). Application of the lower and upper bound theorems of plasticity to collapse of circular foundations. Proc. 10th Int. Conf. of IACMAG, Vol 2., pp. 1417-1428. Tucson.

Nonlinear finite elements/Lagrangian and Eulerian descriptions. (2010, September 2). Retrieved April 23, 2013, from Wikiversity: http://en.wikiversity.org/wiki/Nonlinear_finite_elements/Lagrangian_and_Eulerian_descriptions

Randolph, M.F. & Andersen, K.H. (2006). Numerical analysis of T-bar penetration in soft clay. International journal of geomechanics(6), 411-420.

Randolph, M.F. & Houlsby, G.T. (1984). The limiting pressure on a circular pile loaded laterally in cohesive soil. Geotechnique, 34(4), 613-623.

Stewart, D.P. & Randolph, M.F. (1994). T-bar penetration testing in soft clay. Journal of Geotechnical Engineering(12), 2230-2235.

Tjahyono, S. (2011). Experimental and numerical modelling of spudcan penetration in stiff clay overlying soft clay. PhD Thesis, National university of Singapore, Department of civil engineering, Singapore.

World Fleet of Jack-Up Drilling Rigs. (2012, October 10). Retrieved June 3, 2013, from http://shipbuildinghistory.com/today/highvalueships/offshorejackups.htm